Environmental Science Nano

Accepted Manuscript

ROYAL SOCIETY OF CHEMISTRY

rsc.li/es-nano

Size-dependent cytotoxicity of copper oxide nanoparticles in lung epithelial cells

Amaraporn Wongrakpanich [1,2,3], Imali A. Mudunkotuwa [4], Sean M. Geary [1], Angie S. Morris[1,4], Kranti A. Mapuskar [5], Douglas R. Spitz [5], Vicki H. Grassian [4,6] and Aliasger K. Salem [1]

[1]Department of Pharmaceutical Sciences and Experimental Therapeutics, College of Pharmacy, University of Iowa, Iowa city, IA 52242, United States
[2]Department of Pharmacy, Faculty of Pharmacy, Mahidol University, Bangkok 10400, Thailand
[3]Center of Excellence in Innovative Drug Delivery and Nanomedicine, Faculty of Pharmacy, Mahidol University, Bangkok 10400, Thailand.
[4]Department of Chemistry, University of Iowa, Iowa city, IA 52242, United States
[5]Department of Radiation Oncology, Carver College of Medicine, University of Iowa, Iowa city, IA 52242, United States
[6]Departments of Chemistry and Biochemistry, Nanoengineering and the Scripps Institution of Oceanography, University of California San Diego, 9500 Gilman Dr, La Jolla, CA 92093, United States

Corresponding author: Aliasger K. Salem
College of Pharmacy, University of Iowa
115 S. Grand Avenue, S228 PHAR, Iowa City, IA, 52242, USA
E-mail: aliasger-salem@uiowa.edu

Abstract

The increasing use of copper oxide (CuO) nanoparticles (NPs) in medicine and industry demands an understanding of their potential toxicities. In this study, we compared the *in vitro* cytotoxicity of CuO NPs of two distinct sizes (4 and 24 nm) using the A549 human lung cell line. Despite possessing similar surface and core oxide compositions, 24 nm CuO NPs were significantly more cytotoxic than 4 nm CuO NPs. The difference in size may have affected the rate of entry of NPs into the cell, potentially influencing the amount of intracellular dissolution of Cu^{2+} and causing a differential impact on cytotoxicity.

Keywords

Copper oxide, nanoparticles, toxicity, A549

Nano impact

Cu-based NPs, especially CuO NPs need to be understood in terms of their impact on health and the environment. Of particular concern is their use as antimicrobial agents where susceptibility of target and off-target organisms to the toxic effects of these NPs overlap. We show here that the difference in size of CuO NPs can have a significant impact on cytotoxicity with smaller nanoparticles being less toxic than larger ones.

Introduction

In recent years, engineered NPs have been utilized in many fields, including biomedical sciences, engineering and industry [1]. Aside from the negative impact that these NPs may have on a range of valuable "off-target" non-human life forms [2-4], the increased use of engineered NPs also raises the risk of human exposure, often via the respiratory and gastrointestinal tracts, due to the increased release of these particles into the environment [5, 6]. This raises a concern regarding the possible cytotoxicity and side effects of NPs upon human exposure [7]. Nanoscale particles have very high surface-to-volume ratios when compared to the bulk phase, exhibiting unique physicochemical properties that may render them cytotoxic under certain circumstances[8-11].

CuO NPs contain a single phase, tenorite [12]. They are used for numerous applications in the electronic and optoelectronic industries such as in gas sensors, semiconductors and thin films for solar cells [13-15]. CuO NPs also have desirable traits for many medical applications. Recent work has shown that CuO NPs have microbiocidal activity against both fungi and bacteria [16-20] and have been shown to reduce bacterial biofilm formation [21, 22]. CuO NPs also have a high potential to be used as a MRI-ultrasound dual imaging contrast agent [23]. With these increasing applications, there are many potential routes of exposure to engineered nanomaterials including CuO NPs. For example, Cu-based engineered nanomaterials are active ingredients in marine antifouling paints and agricultural biocides where they can become airborne and finally deposit in soil [24, 25]. Airborne nanomaterials can also be deposited into natural water bodies in addition to their direct release that can result in contaminated water

systems [26, 27]. Furthermore, metallic Cu NPs can be released into the environment from power stations, smelters, metal foundries, asphalt, inkjet printers and rubber tires [28] and can undergo oxidation under ambient conditions forming CuO NPs [29]. Wang *et al.* has shown that dissolved copper in association with CuO NPs are primary redox-active species and the CuO NPs undergo sulfidation by a dissolution-reprecipitation mechanism [30].

In order to employ these metal-based engineered NPs in biomedical applications, their behavior in physiological systems needs to be addressed and fully understood. For example, particle dissolution can occur under biological conditions, specifically in the presence of natural coordinating organic acids, resulting in the release of dissolved metal ions to the surrounding solution. Dissolution can also lead to decreased particle size and in turn increased particle mobility [29, 31, 32]. These are important considerations for the use of NPs in biomedical research because these are factors that could be directly related to cytotoxicity.

There have been several studies conducted to evaluate the toxicity of CuO NPs. Pettibone *et al*. investigated the whole-body inhalation exposure of mice to copper and iron nanoparticles that showed increased inflammatory responses for copper nanoparticles three-weeks post exposure [12]. Karlsson *et al.* conducted a study on different metal oxide nanoparticles (CuO, TiO_2, ZnO, $CuZnFe_2O_4$, Fe_3O_4, Fe_2O_3) and compared their toxicity to multi-walled carbon nanotubes [33]. The results indicated that CuO nanoparticles were the most potent regarding cytotoxicity and DNA damage and it was not entirely attributed to the dissolved ions. In another study by Fahmy *et al.* CuO nanoparticles were observed to overwhelm antioxidant defenses in airway epithelial cells [34]. Heinlaan *et al.* compared the toxicity of nanoscale and bulk CuO, ZnO and TiO_2 using *V. fischeri, D. magna* and *T. platyurus* [35]. The LC_{50} values reported in this study for nanoscale CuO was 50-100 fold lower than for bulk CuO. A recent study by Mancuso et at. highlighted that nanoscale CuO exhibits a nearly 30-fold enhancement in cytotoxicity compared to bulk materials based when testing using human bone marrow mesenchymal stem cells (hBMMSCs) [36]. These studies provide strong evidence of significant differences between the toxicological impacts of CuO particles depending on their particle size. Based on these findings, the nanoscale particles (particles which were approximately 20-50 nm) show considerably higher toxicities than larger micron-sized particles.

Following on these studies, we focus here on further understanding the role of particle size in CuO toxicity and to study size effects for nanoparticles below 100 nm in diameter. In particular, in this study, two sizes of CuO NPs were compared; 1) 4 nm CuO NPs, and 2) 24 nm CuO NPs. The goals of the current study were to compare the cytotoxicity of differently sized CuO NPs and investigate the specific causes of cytotoxicity induced *in vitro* using a human lung cell line as a representative cell type of the respiratory tract [37]. This study attempts to provide insight into the factors that affect the cytotoxicity of CuO NPs.

Materials and methods:

Characterization of Cu-based NPs

The CuO NPs used in this study were extensively characterized for size, surface area, core and surface composition. The average particle sizes of CuO NPs were determined using transmission electron microscopy (JEOL JEM-1230 TEM). Surface areas were measured using

a multipoint Brunauer-Emmett-Teller (BET) surface analyzer (Quantachrome Nova 4200e) using nitrogen as the adsorbent. The bulk and surface compositions were determined using X-ray diffraction (XRD) and X-ray photoelectron spectroscopy (XPS), respectively. Data generated from these characterizations are summarized in Table 1. Large (24 nm) CuO NPs were purchased from Sigma-Aldrich (St. Louis, MO) while small (4 nm) CuO NPs were synthesized in the lab according to the following protocol. A copper-containing precursor, $Cu(OAc)_2$ (1.74 g), was added to 100 mL methanol. The solution was then refluxed for several minutes to dissolve the precursor. Afterwards, 3 mL of water was added to this solution. Upon completely dissolving $Cu(OAc)_2$, a solution of methanol (50 mL) containing 0.7 g of NaOH was added dropwise and further refluxed for 50 hours. The resultant black precipitate was collected by evaporating the methanol on a rotary evaporator followed by multiple washings using acetone (20 mL), water (20 mL) and ethanol (20 mL) respectively. At each washing step, the nanoparticles were collected via centrifugation at 22000 rpm. Finally the collected precipitate was dried in the oven overnight at 106°C and finely ground using a mortar and pestle.

Cell culture

The human alveolar lung adenocarcinoma cell line, A549, was kindly provided by Peter S. Thorne, Department of Occupational and Environmental Health, College of Public Health, University of Iowa. A549 cells were maintained in RPMI-1640 media (Gibco, Life technologies, Grand Island, NY) supplemented with 10% fetal bovine serum (FBS, Atlanta Biologicals, Lawrenceville, GA), 1 mM sodium pyruvate (Gibco), 10 mM HEPES (Gibco), 1 mM Glutamax (Gibco) and 50 µg/mL gentamycin sulfate (IBI Scientific, Peosta, IA). Cells were incubated at 37°C in a 5% CO_2 humidified atmosphere and were shown to be free of mycoplasma.

Cytotoxicity assay

A549 cells were plated 1 day prior to NP treatment in 96-well plates at a concentration of 1×10^4 cells/well. In all cell-based experiments, all treatments (4 nm CuO NPs, 24 nm CuO NPs, $Cu(NO_3)_2$ and $NaNO_3$) were dispersed in media using a sonic dismembrator (Fisher Scientific, Pittsburgh, PA) at 40% amplitude for 1 minute at 1 mg/mL (12.6 mM CuO) before dilution. $Cu(NO_3)_2 \cdot 3H_2O$ and $NaNO_3$ were purchased from Sigma-Aldrich. $Cu(NO_3)_2$ was included in the study in order to evaluate the effect on cell viability of dissolved Cu^{2+} in solution. These two types of CuO NPs and $Cu(NO_3)_2$ were added by normalizing against Cu^{2+} concentration. $NaNO_3$ was used as a negative control for NO_3^{2-} in $Cu(NO_3)_2$. Cells were exposed to different concentrations of Cu^{2+} ranging from 0.06 – 1.57 mM (or 5 – 125 µg/ml CuO) for 1, 4, 24 and 48 h. At the end of the indicated incubation period, the treatment in each well was replaced with 100 µL of fresh media and 20 µL of MTS tetrazolium compound (CellTiter 96® AQ_{ueous} One Solution, Promega, Madison, WI). After 1 - 4 h, the absorbance was recorded at 490 nm using a Spectra Max plus 384 microplate spectrophotometer (Molecular Devices, Sunnyvale, CA). Cell viability was expressed as a percentage of the absorbance value obtained for the untreated cells. All absorbance values were corrected with a blank solution (100 µL of fresh media and 20 µL of MTS tetrazolium compound).

Dissolution of Cu^{2+} from CuO NPs

In separate experiments, nanoparticles (4 nm and 24 nm CuO NPs) were dispersed in complete RPMI-1640 media using a sonic dismembrator at 40% amplitude for 1 minute before dilution. The NP suspensions at different concentrations of Cu^{2+} ranging from 0.06 – 1.57 mM (or 5 – 125 µg/ml CuO) were incubated at 37°C and 5% CO_2 to mimic the same conditions as in cytotoxicity assays. After 4 different time points (1, 4, 24 and 48 h), the NP suspensions were centrifuged at 10016 x *g* for 25 mins to pellet the CuO NPs. Supernatants were collected, diluted in 5 mM HNO_3 and was analyzed via inductively coupled plasma–optical emission spectroscopy (ICP-OES, Varian, Agilent Technologies, Santa Clara., CA) to determine the dissolved Cu^{2+} concentration. In addition, a droplet of the supernatant was placed on a TEM grid and imaged to test the presence of any smaller nanoparticles that could not be removed from the centrifugation process [29].

Measurement of intracellular reactive oxygen species (ROS) production by dihydroethidium (DHE) oxidation

A549 cells were plated in 60 mm^2 dishes at a concentration of 2 x 10^5 cells/dish. Twenty four hours following plating, the cells were treated with 4 mL of 4 nm CuO NPs, 24 nm CuO NPs, $Cu(NO_3)_2$ or $NaNO_3$. The two types of CuO NPs and $Cu(NO_3)_2$ were added such that equal amounts of Cu^{2+} (0.12 µM Cu^{2+} concentration) were added for each treatment. $NaNO_3$ was used as a negative control for NO_3^{2-} in $Cu(NO_3)_2$. Following the 1, 4, 24 or 48 hours treatment, the cells were trypsinized with 0.25% trypsin-EDTA and centrifuged at 230 x *g* for 5 minutes. The cells were washed with PBS containing 5 mM pyruvate and incubated for 40 mins at 37°C with 10 µM of the commercially available dye, dihydroethidium (DHE), in PBS containing pyruvate. Following incubation with the dye, the cells were analyzed using flow cytometry (FACScan: Becton Dickinson Immunocytometry Systems, San Jose, CA). The mean fluorescence intensity (MFI) of 20,000 cells was recorded. All groups were normalized to the untreated control group. Antimycin A (an electron transport chain blocker) which was used as a positive control increased the DHE oxidation levels by 3- to 5-fold (data not shown).

Measurement of mitochondrial ROS production via MitoSOX

A549 cells were seeded at a concentration of 2 x 10^5 cells/well in 60 mm^2 dishes one day prior to treatments. Two different sizes of CuO NPs (4 and 24 nm) and $Cu(NO_3)_2$ were added such that equal amounts of Cu^{2+} (0.12 µM Cu^{2+} concentration) were added for each treatment. $NaNO_3$ was added as a control. At two different time points (1 and 24 hours), cells were removed from dishes by trypsinization, stained with MitoSOX (final concentration 2 µM for 15 minutes) and the fluorescence was measured via flow cytometry. The mean fluorescence intensity (MFI) of 10,000 cells per sample was calculated. All groups were normalized to the control (untreated) group. Antimycin A was used as a positive control and showed a MFI approximately 28-fold greater than the control.

Intracellular Cu^{2+} uptake

A549 cells were seeded at a concentration of 4 x 10^5 cells/well in 60 mm^2 dishes one day prior to treatments. Two different sizes of CuO NPs (4 and 24 nm) and $Cu(NO_3)_2$ were added such that equal amounts of Cu^{2+} were added for each treatment. At 4 different time points (1, 4, 24 and 48 hours), cells were gently washed twice with warm PBS and removed from dishes by trypsinization. Cells were collected and centrifuged at 230 x g for 5 minutes, gently washed once with warm PBS and resuspended in 1 mL complete medium. These repeat

washing cycles were introduced to the experiment to ensure the complete removal of extracellular CuO NPs and Cu^{2+}. A small aliquot (20 µL) of the cell suspension was used to determine cell concentration using a hemocytometer. The rest of the cell suspension was digested with concentrated HNO_3 (3 mL) using microwave digestion (MARS 6, CEM Corporation) and the Cu^{2+} concentration in the digestate was quantified via ICP-OES. The limit of detection for Cu^{2+} using ICP-OES is 5 µg/L. The Cu^{2+} in the digestate was used to calculate the amount of CuO in the cells (assumption: Cu^{2+} in the digestate is due to internalized CuO NPs or Cu^{2+}). The intracellular Cu^{2+} from each sample was normalized against cell number.

Statistical analysis

Data are expressed as mean ± SD. For the cytotoxicity assay, a non-linear regression with second order polynomial (quadratic), least squares fit was used. For all other experiments, One-way ANOVA with Bonferroni's post-test (comparing all groups to the control group and comparing 4 nm with 24 nm CuO NPs) was performed. All statistical analyses were conducted using GraphPad Prism version 6.05 for Windows (GraphPad Software, San Diego, CA, www.graphpad.com). The *p*-values of less than 0.05 were considered significant.

Results and discussion:

CuO NP characterization

The average sizes of the CuO NPs used in these studies were 4 ± 1 nm ("small") and 24 ± 9 nm ("large") (Figure 1). To evaluate the effect of cell culture medium on the overall size of the CuO nanoparticles in our study, we measured the particle size of the CuO (4 nm) nanoparticles in complete media for 0 hrs, 4 hrs and 24 hrs using a Zetasizer Nano ZS at the same concentrations they were tested in the cell viability studies. The average hydrodynamic diameter for the CuO NPs tested was 5.2 ± 0.2 nm (Fig 1S.) which is consistent with the size results from the TEM analysis. RPMI medium did induce moderate levels of aggregation and the overall average particle size was stable over 24 hours. It is worth noting that changing parameters such as ionic strength, nature of buffer, particle size, particle surface composition, and percentage serum in the media can have a significant effect on the degree of aggregation and the effect of these various parameters on aggregation and cell toxicity need further investigation. The Brunauer-Emmett-Teller (BET) surface areas of the small and large CuO NPs were 118 ± 4 m^2/g and 22 ± 0.4 m^2/g, respectively [29]. Bulk phase analysis with X-ray diffraction indicated that both the small and large CuO NPs consisted of a single phase; tenorite and surface analysis using X-ray photoelectron spectroscopy (XPS) revealed that in both particle types the copper atoms are in the same oxidation state (Cu(II)) in the near surface region (Figure 2). These oxide nanoparticles are truncated with OH groups at the surface as indicated by the peak at 531 eV in the O1s region. In addition, the carbon 1s region of the XPS spectrum showed 4 nm CuO NPs had some surface adsorbed acetate groups resulting from the copper acetate precursor used in the synthesis process and 24 nm CuO NPs had some adsorbed carbonates on the surface. These characterization data are summarized in Table 1.

Comparison of cytotoxic effects of 4 nm CuO NPs versus 24 nm CuO NPs on A549 cells

After the particles were dispersed by sonication in RPMI-1640 media, the two differently sized CuO NPs were added to A549 cells at concentrations ranging from 0.06 – 1.57 mM (of Cu^{2+}) for 1, 4, 24 or 48 hours and the percent cell viability (relative to untreated control cells) was determined immediately after each incubation period using an MTS assay. The results (Figure 3) suggest that cytotoxicity yielded from A549 cells were dependent on both time of exposure to, and concentration of, either 4 nm CuO NPs or 24 nm CuO NPs. In addition, it was also noted that, at 1, 4, 24 and 48 h time points, there were significant differences (p-value < 0.05 for 1 h, p-value < 0.001 for 4, 24 and 48 h) in percent cell viability of A549 cells after treatment with 4 nm CuO NPs versus 24 nm CuO NPs. In short, it was apparent that 24 nm CuO NPs exhibited higher cytotoxicity compared to 4 nm CuO NPs. The higher cytotoxicity was particularly evident at 4 h, 24 h and 48 h and when concentrations of loaded Cu were 0.94 – 1.57 mM, 0.31 – 1.57 mM and 0.31 – 0.94 mM, respectively.

Effect of dissolved Cu^{2+} ions on A549 cytotoxicity

$Cu(NO_3)_2$ was used as a treatment alongside solid CuO NPs in order to determine the effect of dissolved Cu^{2+} on cell viability. $NaNO_3$ was used as a negative control to confirm that nitrate ions had no cytotoxic effects and that any decrease in cell viability can instead be attributed to Cu^{2+} in solution. There was no impact on cell viability due to treatment with $NaNO_3$ relative to untreated cells at any time point or at any concentration (data not shown). However, the introduction of free Cu^{2+} from $Cu(NO_3)_2$ demonstrated both time- and concentration-dependent cytotoxicity in A549 cells. Cells treated with free Cu^{2+} demonstrated lower cell viability than cells treated with 4 nm CuO NPs but showed higher cell viability than cells treated with 24 nm CuO NPs (Figure 3). This was apparent at 4, 24 and 48 h incubation periods.

In an attempt to investigate the underlying cause of CuO NP cytotoxicity, the dissolution of Cu^{2+} from the two differently sized CuO NPs was measured using ICP-OES after the particles were sonicated with RPMI-1640 media and incubated at 37°C, 5% CO_2 for 1, 4, 24 and 48 h (Figure 4). Three concentrations of CuO NPs (0.06, 0.63 and 1.57 mM) were chosen to represent the range of concentrations tested in the cytotoxicity assay. Because the TEM analysis of the supernatant did not show any particle presence, the concentrations obtained using ICP-OES can be attributed entirely to dissolved Cu^{2+}. In another study, where CuO NP dissolution was tested in the presence of citric and oxalic acid, the concentrations reported by ICP-OES consisted of both dissolved and smaller CuO nanoparticles [29]. The concentration of free Cu^{2+} in the media increased as the initial concentration of 4 nm and 24 nm CuO NPs in the media increased. For all concentrations tested the complete dissolution of Cu^{2+} from either type of NPs was not observed after 48 h. Both types of CuO NPs released Cu^{2+} at similar levels at 24 and 48 h which is approximately 50% of the original concentrations. However, the rates of free Cu^{2+} dissolution were different. Smaller 4 nm CuO NPs achieved ~50% dissolution into the surrounding medium over a 1 h incubation period. Larger 24 nm CuO NPs took longer to reach ~50% Cu^{2+} dissolution (over 24 h). Thus, 4 nm CuO NPs had a faster extracellular Cu^{2+} dissolution rate when compared to 24 nm CuO NPs.

That there is a direct relationship between the degree of cytotoxicity and the concentration of soluble extracellular Cu^{2+} after 24/48 hours of exposure (Figure 3) suggests that free Cu^{2+} in solution is likely to be one of the major causes of cytotoxicity seen with the

small NPs used in these studies. In fact, free Cu^{2+} ions may have contributed to most of the cytotoxicity caused by the 4 nm Cu NPs. This preliminary assessment is based on the finding that the 4 nm CuO NPs released approximately 50% of their total loaded Cu as Cu^{2+} at 1 hour (Figure 4) and were less cytotoxic than the soluble $Cu(NO_3)$ exposed to the A549 cells at twice the concentration (for the 24 and 48 hour treatments), tentatively indicating at this stage that other factors were negligible in causing cytotoxicity. However, it appears to be a different situation for the 24 nm CuO NPs where it is likely that other or, more likely, additional factors may have contributed to the cellular cytotoxicity caused by these NPs aside from the extracellular release of Cu^{2+} ions. This is because 24 nm CuO NPs caused greater cytotoxicity than 4 nm CuO NPs despite the finding that 4 nm NPs had a faster Cu^{2+} dissolution profile than 24 nm CuO NPs. Also, the 24 nm CuO NPs were significantly more toxic than soluble Cu^{2+} from $Cu(NO_3)$ which was exposed to cells at more than twice the concentration of soluble Cu^{2+} released by the CuO NPs.

Evaluation of intracellular and mitochondrial pro-oxidants induced by CuO NPs

Intracellular prooxidant levels (intracellular $O_2^{\bullet-}$) in A549 cells after treatment with 4 nm or 24 nm CuO NPs for 1, 4, 24 or 48 h were assessed through the detection of DHE oxidation, which is indicative of superoxide anions ($O_2^{\bullet-}$) as well as other prooxidants. The results demonstrated that, at 1 h and 4 h (Figure 5A and 5B), there was a significant drop in prooxidant levels in cells treated with 24 nm CuO NPs which was not observed for the other treatments, including the 4 nm CuO NPs treatment. This finding for the 24 nm CuO NPs is possibly due to antioxidant defense mechanisms induced in the A549 cells in response to a metal-based NP challenge and has been shown to occur at 4 – 8 hours post-treatment in a previously published study where A549 cells were characterized for prooxidant levels after treatment with CuO NPs [38, 39]. When prooxidants were measured at 24 h and 48 h (Figure 5C and 5D) there were significant increases (2-fold and 4-fold, respectively) in the cells that were treated with 24 nm CuO NPs compared to controls ($p < 0.001$), possibly due to exhaustion of the antioxidant defense system. In comparison, cells treated with 4 nm CuO NPs over 24 h and 48 h did not exhibit a significant increase in prooxidant levels compared to untreated cells. When 4 nm and 24 nm CuO NPs were compared, cells that were treated with 24 nm CuO NPs over 24 h and 48 h exhibited significantly higher levels of prooxidants when compared with cells that were treated with 4 nm CuO NPs ($p < 0.001$). Cells treated with free Cu^{2+} produced 2-fold higher levels of prooxidants at 24 h and 48 h than untreated cells. Overall, these results are consistent with the cytotoxicity assays (Figure 3) and confirm that 24 nm CuO NPs were more toxic when compared to free Cu^{2+} and 4 nm CuO NPs. It is possible that differences in prooxidant levels account for differences in cytotoxicity (Figure 3) observed when comparing 24 nm CuO NPs with $Cu(NO_3)$.

Since it has been shown that CuO NPs at sizes of < 40 nm can enter mitochondria of A549 cells within 12 h of incubation [39], mitochondrial superoxide production was measured in variously treated A549 cells using MitoSOX red [40]. Two incubation periods (1 h and 24 h) were tested. It was found that at 1 h, there were no substantive differences when comparing 24 nm CuO NPs with either the untreated control or the group treated with 4 nm CuO NPs (Figure 6A). At 24 h, cells that were treated with 24 nm CuO NPs had significantly more mitochondrial

superoxide (12-fold higher than the control group) ($p < 0.001$ when compared to control and 4 nm CuO NPs). Cells that were treated with $Cu(NO_3)_2$ had 1.6-fold higher levels of mitochondrial ROS than the untreated cells. Mitochondrial ROS level in cells that were treated with 4 nm CuO NPs was at the same level as in untreated cells (MFI equals to 1) (Figure 6B). Treatment of cells with $NaNO_3$ showed no significant change when compared to the untreated cells at both incubation periods. The results obtained here and with the intracellular superoxide measurements performed above demonstrate that 24 nm CuO NPs induced higher mitochondrial and intracellular ROS than 4 nm CuO NPs and this difference in ROS production was likely to be another major cause of cytotoxicity for cells treated with the 24 nm CuO NPs.

Quantification of the intracellular Cu^{2+} from cells that were treated with 4 nm and 24 nm CuO NPs

Both types of NPs studied here possessed similar surface and core oxide compositions (Figure 2) and the smaller 4 nm CuO NPs exhibited faster extracellular Cu^{2+} dissolution rates than the larger 24 nm CuO NPs (Figure 4), leading us to suspect that 4 nm CuO NPs may have been more cytotoxic than 24 nm CuO NPs. However, results from the MTS assays (Figure 3) showed that 24 nm CuO NPs were significantly more cytotoxic than 4 nm CuO NPs. This was particularly evident at 24 and 48 h for the lower Cu concentrations (Figure 3). Therefore, there are likely to be other factors, aside from Cu^{2+} dissolution rates, that contribute to the increased cytotoxicity of 24 nm CuO NPs. It is possible that these two types of NPs have different modes of entry or rates of uptake because of their difference in size, which consequently may affect the levels of Cu^{2+} accumulating within the cells.

To study the possibility of different modes of entry or rates of uptake depending on the particle size, cells were incubated with 4 nm, 24 nm CuO NPs and $Cu(NO_3)_2$ for a range of times (1, 4, 24 and 48 h), and then intracellular Cu^{2+} was measured using ICP-OES (Figure 7). In this experiment, cell suspensions were subjected to microwave digestion with concentrated HNO_3 thus; this intracellular Cu^{2+} that was detected via ICP-OES could come from either free Cu^{2+} or CuO in particulate form. At all incubation periods, the only group demonstrating relatively high intracellular Cu^{2+} was the one where the cells were treated with 24 nm CuO NPs ($p < 0.001$). Cells that were treated with 4 nm CuO NPs or $Cu(NO_3)_2$ showed low intracellular Cu^{2+} concentrations compared to the cells treated with 24 nm CuO NPs. These results suggest that 24 nm Cu NPs are more rapidly and more efficiently taken up by A549 cells that 4 nm CuO NPs.

There have been numerous reports on the cytotoxicity of CuO NPs both *in vivo* and *in vitro* [36, 41-45]. There is still, however, a large degree of conjecture as to the mechanism(s) by which these NPs mediate their cytotoxicity. These differences are likely to stem from multiple variables between studies including the cell type studied and the properties of the particles used. This is further confounded by the possibility that multiple mechanisms may be responsible for nanotoxicity of CuO NPs as opposed to one major causative factor.

Previous studies addressing CuO NPs toxicity showed that among various metal oxide NPs, CuO NPs were among the most cytotoxic [33, 45]. Also, CuO NPs have higher cytotoxicity

when compared with CuO microparticles [28, 46, 47]. However, to the best of our knowledge, comparisons in toxicity of CuO NPs at the very small sizes used here have not been previously reported in the literature. Here, we measured and observed the differences in cytotoxicity of two groups of differently sized CuO NPs (4 nm and 24 nm). Surprisingly, the larger CuO NPs (24 nm) demonstrated higher cytotoxicity as well as inducing higher intracellular and mitochondrial ROS production than the smaller CuO NPs (4 nm), despite both groups of NPs having identical chemical compositions and the 4 nm CuO NPs showing faster extracellular Cu^{2+} dissolution rates. Interestingly, cells treated with 24 nm CuO NPs showed comparatively high intracellular Cu^{2+} (Figure 7). This disparity in intracellular Cu^{2+} levels was likely due to the larger volumes (> 200-fold) of 24 nm NPs over 4 nm NPs. To a less significant degree, it is also possible that the rates of NP uptake were different, with uptake being slower for the 4 nm CuO NPs. The rate of entry and amount of uptake of CuO NPs into the cell may have ultimately affected the level of intracellular accumulation of Cu^{2+} and consequently impacted on cytotoxicity in A549 cells. CuO NPs have been previously shown to rely on endocytosis to enter A549 cells [39]. Entry into acidic compartments (e.g. endolysosomes) results in exposure to a lower pH environment and it has been demonstrated that CuO NPs release Cu^{2+} more rapidly at lower pH [6, 31]. It may be that smaller 4 nm CuO NPs used here were not taken up by endocytosis as readily as 24 nm CuO NPs, perhaps due to their smaller diameter, which is substantially below the optimal size to trigger endocytosis, and may have relied upon an inefficient route of entry such as diffusion across the cell membrane [48]. Such a situation, combined with the large volume differences, could have resulted in significant differences in intracellular Cu^{2+} levels and impacted on cytotoxicity through mechanisms dependent on ROS generation, although additional contributions to cytotoxicity through ROS–independent pathways cannot be ruled out, such as the inactivation of vital proteins through chelation or the inactivation of metalloproteins [6]. Based on our findings it is likely that the two differently sized CuO NPs investigated here imparted their cytotoxic effects through mostly disparate mechanisms. The smaller (4 nm) and less toxic CuO NPs are likely to have impacted on cytotoxicity through an undefined pathway caused by the extracellular release of Cu^{2+} which occurred at a faster rate compared to the larger (24 nm) CuO NPs, whilst the larger CuO NPs appeared to have mediated their higher cytotoxic impact through the promotion of greater intracellular and mitochondria ROS levels as a result of increased intracellular access.

Conclusion

Exposure of A549 cells to 4 nm versus 24 nm CuO NPs was performed to assess their cytotoxicity and multiple techniques were performed in an attempt to verify the potential causes of cell death. As a general conclusion, we found that NP-induced cell death may be a result of multiple contributing and confounding factors, however, the predominant causal factor appeared to be dependent on the size of the CuO NPs. We conclude that the extracellular dissolution of Cu^{2+} ions from CuO NPs can be cytotoxic to A549 cells and this seemed to be the primary reason for the cytotoxicity generated by the 4 nm CuO NPs. Despite having similar physicochemical properties (aside from size), the larger 24 nm CuO NPs proved to be significantly more cytotoxic than smaller 4 nm CuO NPs and we can surmise that this was due to post-internalization events resulting in significantly enhanced levels of prooxidants. Evaluating the cytotoxicity of CuO NPs is essential in order to address the safety of using such

materials in biomedical applications where there is the potential for environmental and human exposure. Further evaluation of subtle differences in CuO NP physicochemical properties and the effect of those subtle differences on intracellular behavior and how they impact on cytotoxicity of off-target organisms is warranted and would be of benefit to further understand the potential and limitations of translational and human health applications of copper oxide NPs.

Acknowledgement: This project was supported by the National Institute for Environmental Health Sciences through the University of Iowa Environmental Health Sciences Research Center, NIEHS/NIH P30 ES005605. We thank Katherine S. Waters, Histology Director of the Central Microscopy Research Facility at the University of Iowa and the Radiation and Free Radical Research Core Lab/ P30-CA086862 for technical support and the Lyle and Sharon Bighley Professorship. A. Wongrakpanich would like to thank the Office of the Higher Education Commission and Mahidol University under the National Research Universities Initiative for the support.

References

1. Mody, V. V.; Siwale, R.; Singh, A.; Mody, H. R., Introduction to metallic nanoparticles. *J Pharm Bioallied Sci* **2010,** 2, (4), 282-9.
2. Nowack, B.; Bucheli, T. D., Occurrence, behavior and effects of nanoparticles in the environment. *Environmental Pollution* **2007,** 150, (1), 5-22.
3. Ju-Nam, Y.; Lead, J. R., Manufactured nanoparticles: An overview of their chemistry, interactions and potential environmental implications. *Science of The Total Environment* **2008,** 400, (1–3), 396-414.
4. Buzea, C.; Pacheco, I.; Robbie, K., Nanomaterials and nanoparticles: Sources and toxicity. *Biointerphases* **2007,** 2, (4), MR17-MR71.
5. Worthington, K. L.; Adamcakova-Dodd, A.; Wongrakpanich, A.; Mudunkotuwa, I. A.; Mapuskar, K. A.; Joshi, V. B.; Allan Guymon, C.; Spitz, D. R.; Grassian, V. H.; Thorne, P. S.; Salem, A. K., Chitosan coating of copper nanoparticles reduces in vitro toxicity and increases inflammation in the lung. *Nanotechnology* **2013,** 24, (39), 395101.
6. Chang, Y.-N.; Zhang, M.; Xia, L.; Zhang, J.; Xing, G., The Toxic Effects and Mechanisms of CuO and ZnO Nanoparticles. *Materials* **2012,** 5, (12), 2850.
7. Grillo, R.; Rosa, A. H.; Fraceto, L. F., Engineered nanoparticles and organic matter: A review of the state-of-the-art. *Chemosphere* **2015,** 119, (0), 608-619.
8. Buzea, C.; Pacheco, II; Robbie, K., Nanomaterials and nanoparticles: sources and toxicity. *Biointerphases* **2007,** 2, (4), MR17-71.
9. Elsaesser, A.; Howard, C. V., Toxicology of nanoparticles. *Advanced Drug Delivery Reviews* **2012,** 64, (2), 129-137.
10. Schrand, A. M.; Rahman, M. F.; Hussain, S. M.; Schlager, J. J.; Smith, D. A.; Syed, A. F., Metal-based nanoparticles and their toxicity assessment. *Wiley Interdiscip Rev Nanomed Nanobiotechnol* **2010,** 2, (5), 544-68.
11. Oberdörster, G.; Oberdörster, E.; Oberdörster, J., Nanotoxicology: An emerging discipline evolving from studies of ultrafine particles. *Environmental Health Perspectives* **2005,** 113, (7), 823-839.

12. Pettibone, J. M.; Adamcakova-Dodd, A.; Thorne, P. S.; O'Shaughnessy, P. T.; Weydert, J. A.; Grassian, V. H., Inflammatory response of mice following inhalation exposure to iron and copper nanoparticles. *Nanotoxicology* **2008,** 2, (4), 189-204.
13. Klinbumrung, A.; Thongtem, T.; Thongtem, S., Characterization and gas sensing properties of CuO synthesized by DC directly applying voltage. *Applied Surface Science* **2014,** 313, (0), 640-646.
14. El-Trass, A.; ElShamy, H.; El-Mehasseb, I.; El-Kemary, M., CuO nanoparticles: Synthesis, characterization, optical properties and interaction with amino acids. *Applied Surface Science* **2012,** 258, (7), 2997-3001.
15. Karthick Kumar, S.; Suresh, S.; Murugesan, S.; Raj, S. P., CuO thin films made of nanofibers for solar selective absorber applications. *Solar Energy* **2013,** 94, (0), 299-304.
16. Laha, D.; Pramanik, A.; Laskar, A.; Jana, M.; Pramanik, P.; Karmakar, P., Shape-dependent bactericidal activity of copper oxide nanoparticle mediated by DNA and membrane damage. *Materials Research Bulletin* **2014,** 59, (0), 185-191.
17. Abboud, Y.; Saffaj, T.; Chagraoui, A.; El Bouari, A.; Brouzi, K.; Tanane, O.; Ihssane, B., Biosynthesis, characterization and antimicrobial activity of copper oxide nanoparticles (CONPs) produced using brown alga extract (Bifurcaria bifurcata). *Appl Nanosci* **2014,** 4, (5), 571-576.
18. Thekkae Padil, V. V.; Cernik, M., Green synthesis of copper oxide nanoparticles using gum karaya as a biotemplate and their antibacterial application. *Int J Nanomedicine* **2013,** 8, 889-98.
19. Pelgrift, R. Y.; Friedman, A. J., Nanotechnology as a therapeutic tool to combat microbial resistance. *Advanced Drug Delivery Reviews* **2013,** 65, (13–14), 1803-1815.
20. Yoosefi Booshehri, A.; Wang, R.; Xu, R., Simple method of deposition of CuO nanoparticles on a cellulose paper and its antibacterial activity. *Chemical Engineering Journal* **2015,** 262, 999-1008.
21. Agarwala, M.; Choudhury, B.; Yadav, R. N., Comparative study of antibiofilm activity of copper oxide and iron oxide nanoparticles against multidrug resistant biofilm forming uropathogens. *Indian J Microbiol* **2014,** 54, (3), 365-8.
22. Murthy, P. S.; Venugopalan, V. P.; Das, D. A.; Dhara, S.; Pandiyan, R.; Tyagi, A. K. In *Antibiofilm activity of nano sized CuO*, Nanoscience, Engineering and Technology (ICONSET), 2011 International Conference on, 28-30 Nov. 2011, 2011; 2011; pp 580-583.
23. Perlman, O.; Weitz, I. S.; Azhari, H., Copper oxide nanoparticles as contrast agents for MRI and ultrasound dual-modality imaging. *Physics in Medicine and Biology* **2015,** 60, (15), 5767-5783.
24. Conway, J. R.; Adeleye, A. S.; Gardea-Torresdey, J.; Keller, A. A., Aggregation, Dissolution, and Transformation of Copper Nanoparticles in Natural Waters. *Environmental science & technology* **2015,** 49, (5), 2749-2756.
25. Tegenaw, A.; Tolaymat, T.; Al-Abed, S.; El Badawy, A.; Luxton, T.; Sorial, G.; Genaidy, A., Characterization and potential environmental implications of select Cu-based fungicides and bactericides employed in U.S. markets. *Environmental science & technology* **2015,** 49, (3), 1294-302.
26. Garner, K. L.; Keller, A. A., Emerging patterns for engineered nanomaterials in the environment: a review of fate and toxicity studies. *J Nanopart Res* **2014,** 16, (8), 1-28.
27. Nowack, B.; David, R. M.; Fissan, H.; Morris, H.; Shatkin, J. A.; Stintz, M.; Zepp, R.; Brouwer, D., Potential release scenarios for carbon nanotubes used in composites. *Environment international* **2013,** 59, 1-11.
28. Midander, K.; Cronholm, P.; Karlsson, H. L.; Elihn, K.; Moller, L.; Leygraf, C.; Wallinder, I. O., Surface characteristics, copper release, and toxicity of nano- and micrometer-sized copper and copper(II) oxide particles: a cross-disciplinary study. *Small* **2009,** 5, (3), 389-99.
29. Mudunkotuwa, I. A.; Pettibone, J. M.; Grassian, V. H., Environmental implications of nanoparticle aging in the processing and fate of copper-based nanomaterials. *Environmental science & technology* **2012,** 46, (13), 7001-10.

30. Wang, Z.; von dem Bussche, A.; Kabadi, P. K.; Kane, A. B.; Hurt, R. H., Biological and environmental transformations of copper-based nanomaterials. *ACS nano* **2013,** 7, (10), 8715-27.
31. Elzey, S.; Grassian, V. H., Nanoparticle dissolution from the particle perspective: insights from particle sizing measurements. *Langmuir : the ACS journal of surfaces and colloids* **2010,** 26, (15), 12505-8.
32. Jin, Y.; Zhao, X., Cytotoxicity of Photoactive Nanoparticles. In *Safety of Nanoparticles*, Webster, T. J., Ed. Springer New York: 2009; pp 19-31.
33. Karlsson, H. L.; Cronholm, P.; Gustafsson, J.; Moller, L., Copper oxide nanoparticles are highly toxic: a comparison between metal oxide nanoparticles and carbon nanotubes. *Chem Res Toxicol* **2008,** 21, (9), 1726-32.
34. Fahmy, B.; Cormier, S. A., Copper oxide nanoparticles induce oxidative stress and cytotoxicity in airway epithelial cells. *Toxicology in Vitro* **2009,** 23, (7), 1365-1371.
35. Heinlaan, M.; Ivask, A.; Blinova, I.; Dubourguier, H. C.; Kahru, A., Toxicity of nanosized and bulk ZnO, CuO and TiO2 to bacteria Vibrio fischeri and crustaceans Daphnia magna and Thamnocephalus platyurus. *Chemosphere* **2008,** 71, (7), 1308-16.
36. Mancuso, L.; Cao, G., Acute toxicity test of CuO nanoparticles using human mesenchymal stem cells. *Toxicology mechanisms and methods* **2014,** 24, (7), 449-54.
37. Sahu, S. C.; Casciano, D. A., *Nanotoxicity: From In Vivo and In Vitro Models to Health Risks*. Wiley: 2009.
38. Shi, X.; Castranova, V.; Vallyathan, V.; Perry, W. G., *Molecular Mechanisms of Metal Toxicity and Carcinogenesis*. Springer US: 2012.
39. Wang, Z.; Li, N.; Zhao, J.; White, J. C.; Qu, P.; Xing, B., CuO nanoparticle interaction with human epithelial cells: cellular uptake, location, export, and genotoxicity. *Chem Res Toxicol* **2012,** 25, (7), 1512-21.
40. Mukhopadhyay, P.; Rajesh, M.; Yoshihiro, K.; Haskó, G.; Pacher, P., Simple quantitative detection of mitochondrial superoxide production in live cells. *Biochemical and biophysical research communications* **2007,** 358, (1), 203-208.
41. Melegari, S. P.; Perreault, F.; Costa, R. H.; Popovic, R.; Matias, W. G., Evaluation of toxicity and oxidative stress induced by copper oxide nanoparticles in the green alga Chlamydomonas reinhardtii. *Aquat Toxicol* **2013,** 143, 431-40.
42. Rossetto, A. L.; Melegari, S. P.; Ouriques, L. C.; Matias, W. G., Comparative evaluation of acute and chronic toxicities of CuO nanoparticles and bulk using Daphnia magna and Vibrio fischeri. *The Science of the total environment* **2014,** 490, 807-14.
43. Isani, G.; Falcioni, M. L.; Barucca, G.; Sekar, D.; Andreani, G.; Carpenè, E.; Falcioni, G., Comparative toxicity of CuO nanoparticles and CuSO4 in rainbow trout. *Ecotoxicology and Environmental Safety* **2013,** 97, 40-46.
44. Dai, L.; Banta, G. T.; Selck, H.; Forbes, V. E., Influence of copper oxide nanoparticle form and shape on toxicity and bioaccumulation in the deposit feeder, Capitella teleta. *Marine environmental research* **2015**.
45. Ivask, A.; Titma, T.; Visnapuu, M.; Vija, H.; Kakinen, A.; Sihtmae, M.; Pokhrel, S.; Madler, L.; Heinlaan, M.; Kisand, V.; Shimmo, R.; Kahru, A., Toxicity of 11 Metal Oxide Nanoparticles to Three Mammalian Cell Types In Vitro. *Current topics in medicinal chemistry* **2015,** 15, (18), 1914-29.
46. Semisch, A.; Ohle, J.; Witt, B.; Hartwig, A., Cytotoxicity and genotoxicity of nano - and microparticulate copper oxide: role of solubility and intracellular bioavailability. *Particle and fibre toxicology* **2014,** 11, 10.
47. Karlsson, H. L.; Gustafsson, J.; Cronholm, P.; Moller, L., Size-dependent toxicity of metal oxide particles--a comparison between nano- and micrometer size. *Toxicol Lett* **2009,** 188, (2), 112-8.

48. Gao, H.; Shi, W.; Freund, L. B., Mechanics of receptor-mediated endocytosis. *Proceedings of the National Academy of Sciences of the United States of America* **2005,** 102, (27), 9469-74.

Table 1: Summary of physicochemical characterization data of CuO nanoparticles.

Physicochemical property	Technique	Small CuO NPs	Large CuO NPs
Particle size (nm)	TEM*	4 ± 1	24 ± 9
Surface area (m^2/g)	BET**	118 ± 4	22 ± 0.4
Bulk composition	XRD	CuO	CuO
Surface composition	XPS	Cu-OH, acetate	Cu-OH, carbonate

*Particle size obtained from TEM technique was expressed as mean ± SD and based on 100 particles.
**Surface area obtained from BET technique was expressed as mean ± SD (n=3).

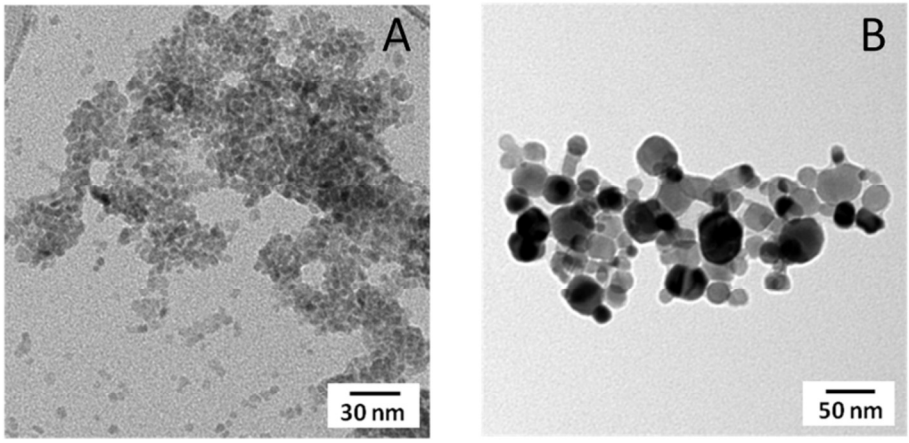

Figure 1: Transmission Electron Microscopy (TEM) images representing small (A) and large (B) CuO NPs which were used in this study. The average particle sizes of small and large CuO NPs, as determined using TEM, were 4 ± 1 nm and 24 ± 9 nm, respectively.

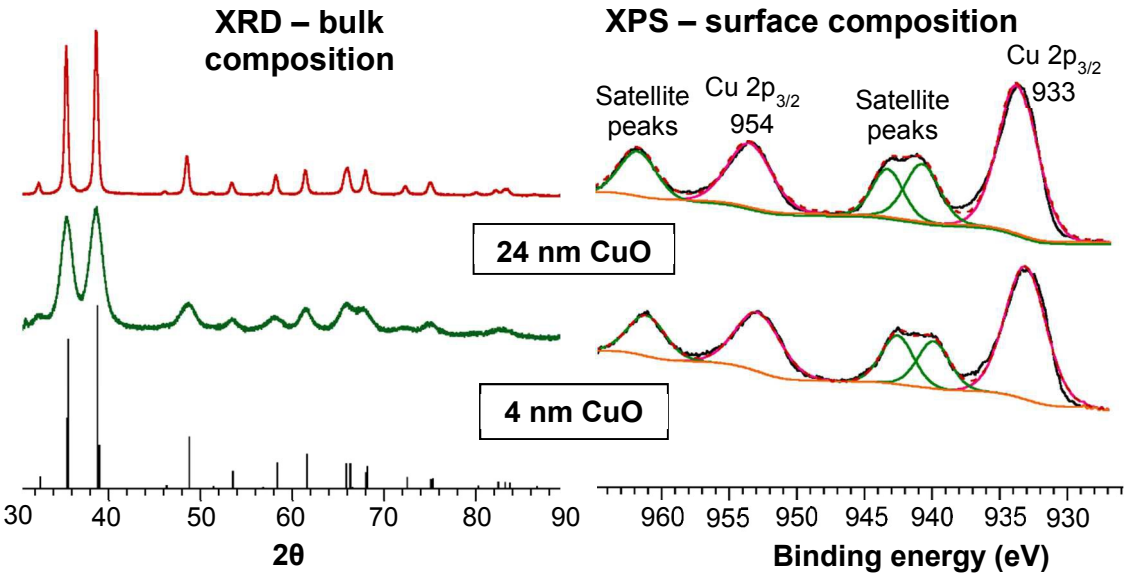

Figure 2: Bulk (left) and surface (right) characterization of small (4 nm) and large (24 nm) CuO NPs using X-ray diffraction (XRD) and X-ray photoelectron spectroscopy (XPS).

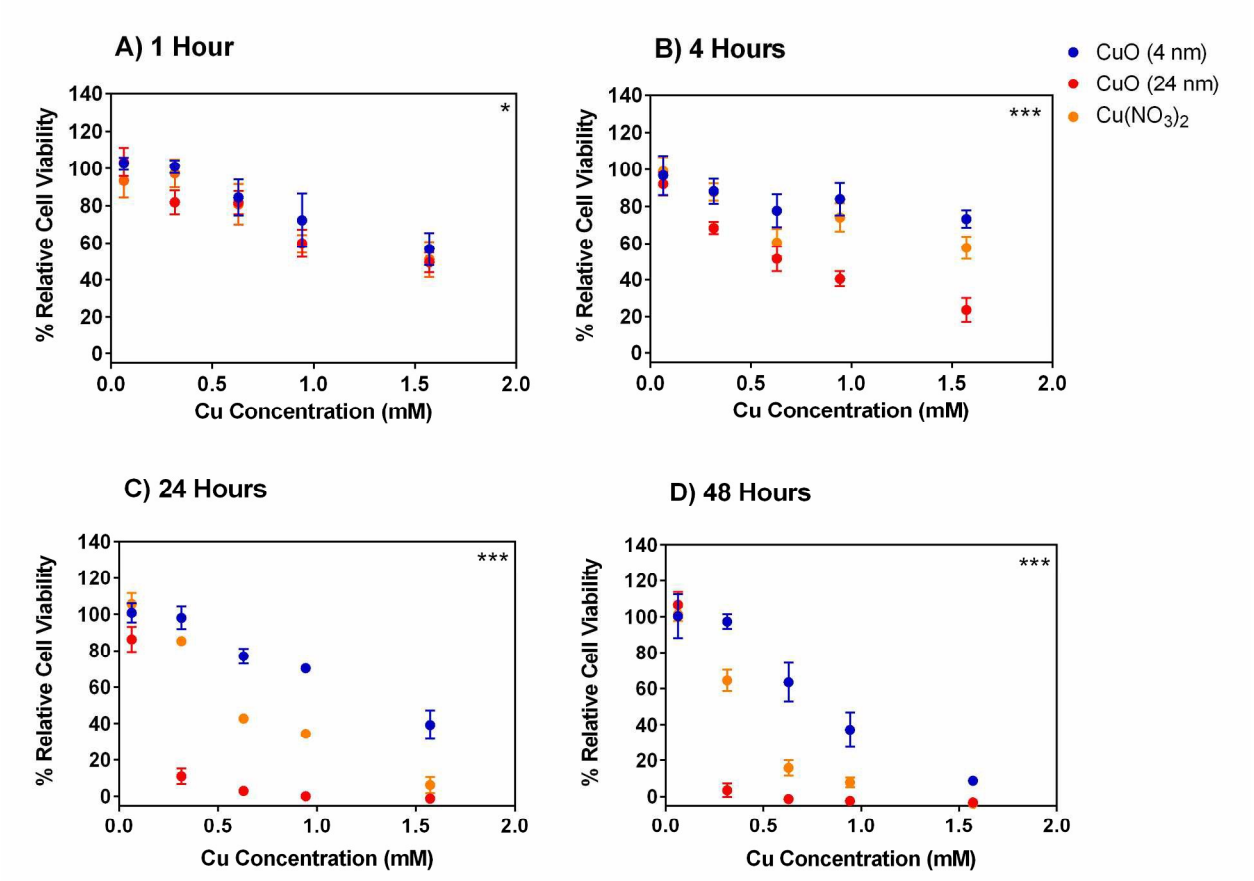

Figure 3: Cytotoxicity of 4 nm versus 24 nm CuO NPs: relative cell viability (%) of A549 cells after treatment with various concentrations of small and large CuO nanoparticles, $Cu(NO_3)_2$ solution and $NaNO_3$ solution for A) 1 hours, B) 4 hours, C) 24 hours and D) 48 hours. The data were plotted according to concentration (mM) and expressed as mean ± SD (n = 3-4). $NaNO_3$ was used as a control for nitrate effects and showed minimal cytotoxicity at all concentrations and all time points tested with relative cell viability > 95% (data no shown). Nonlinear regression, second order polynomial (quadratic), least squares fit were conducted to determine significant differences between 4 nm and 24 nm CuO NP treatments. *** $p < 0.001$, * $p < 0.05$

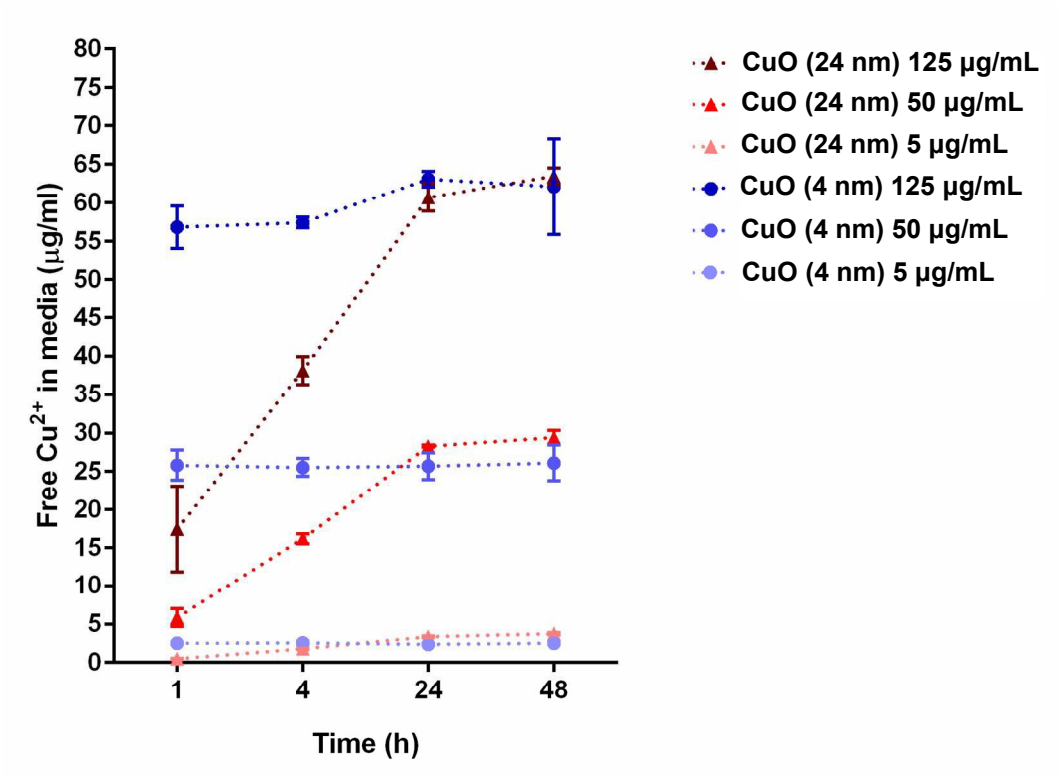

Figure 4: Dissolution of Cu^{2+} from small and large CuO NPs: different concentrations of particles (5, 50 and 125 µg/ml which are equal to 0.06, 0.63 and 1.57 mM, respectively) were sonicated at 40% amplitude for 1 min and then incubated in RPMI-1640 complete media for 1, 4, 24 and 48 h. The data were plotted using free Cu^{2+} in media against time and expressed as mean ± SD (n = 3).

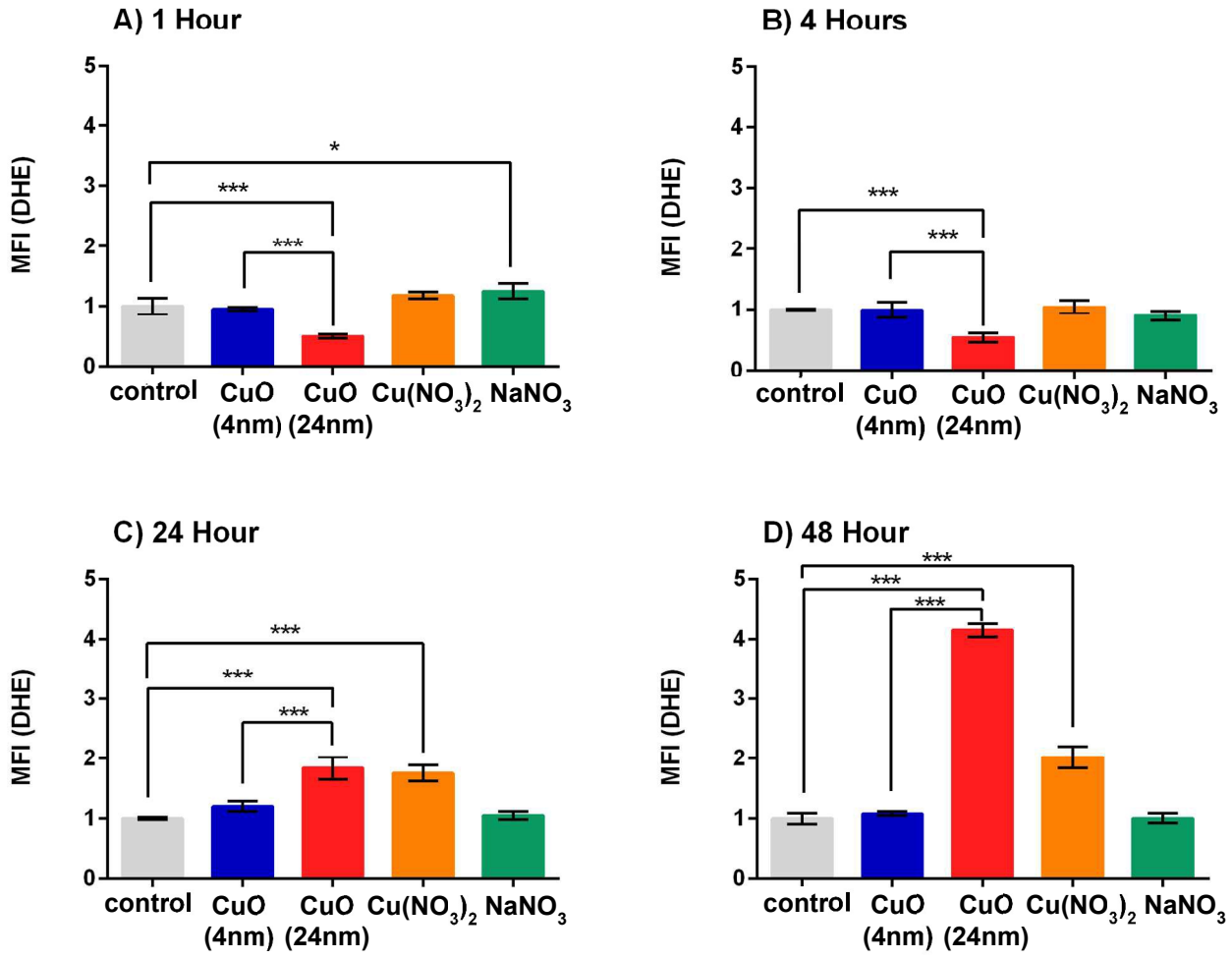

Figure 5: Intracellular pro-oxidants as detected by dihydroethidium oxidation (DHE): cells were incubated with small and large CuO NPs, $Cu(NO_3)_2$ and $NaNO_3$ at a dose of 0.12 µM Cu^{2+} concentration (10 µg/ml CuO NPs) for 1 h (A), 4 h (B), 24 h (C) and 48 h (B). Antimycin A increased the MFI by 3- to 5-fold when compared to the control group (data not shown). MFI represents mean fluorescence intensity which was normalized to the control group. Data are expressed as mean ± SD (n = 3). One-way analysis of variance with Bonferroni's multiple comparisons post-test was performed. *** $p < 0.001$, * $p < 0.05$.

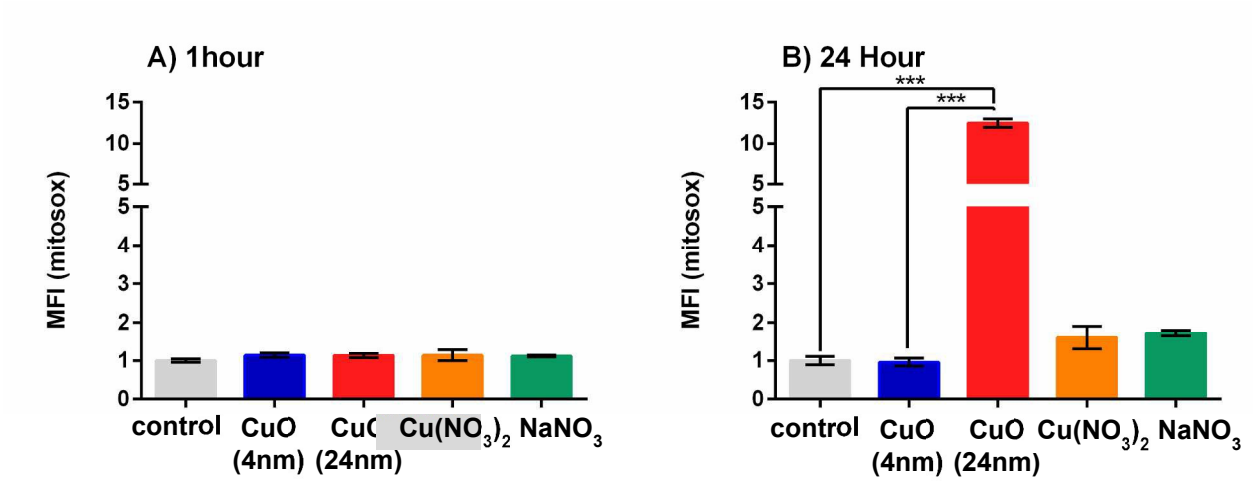

Figure 6: Mitochondrial pro-oxidants as detected by MitoSOX oxidation: cells were incubated with 4 nm and 24 nm CuO NPs, $Cu(NO_3)_2$ and $NaNO_3$ at a dose of 0.12 μM Cu^{2+} concentration (10 μg/ml CuO NPs) for 1 h (A) and 24 h (B). Antimycin A increased the MFI by 10- to 16-fold when compared to the control group at 1 hour and 24 hours, respectively (data not shown). MFI represents mean fluorescence intensity which was normalized to the control group. Data are expressed as mean ± SD (n = 3-5). One-way analysis of variance with Bonferroni's multiple comparisons post-test (the comparison between all groups to the control and between small - large CuO NPs) was performed. *** $p < 0.001$, * $p < 0.05$.

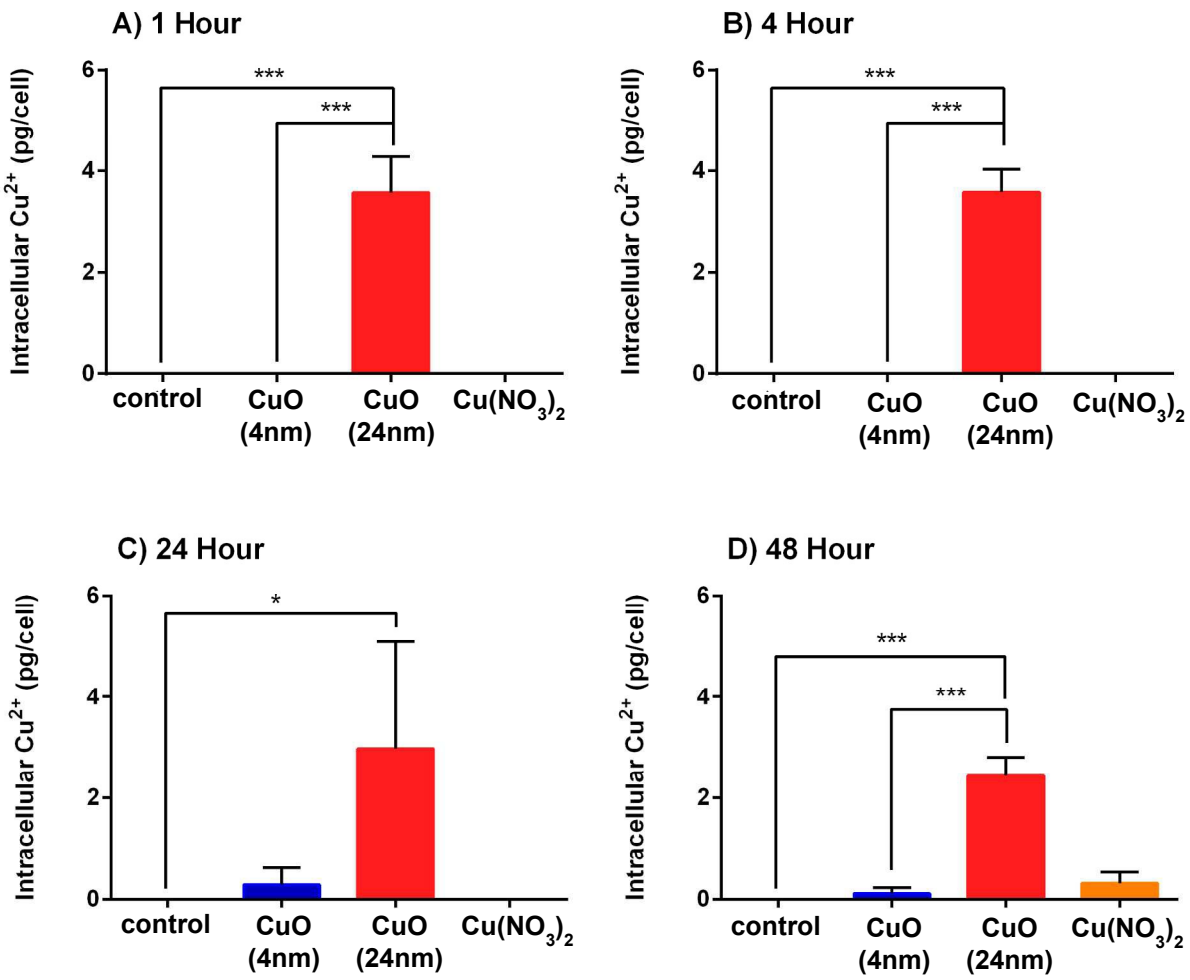

Figure 7: Intracellular Cu^{2+} uptake: cells were incubated with 4 nm and 24 nm CuO NPs, $Cu(NO_3)_2$ and $NaNO_3$ at a dose of 0.12 μM Cu^{2+} concentration (10 μg/ml CuO NPs) for 1 h (A), 4 h (B), 24 h (C) and 48 h (D). Data are expressed as mean ± SD (n = 3). One-way analysis of variance with Bonferroni's multiple comparisons post-test (the comparison between all groups to the control and between 4nm and 24 nm CuO NPs) was performed. *** $p < 0.001$, * $p < 0.05$.